invited review article for the international symposium **"Penetrating Bars Through Masks of Cosmic Dust"** (Johannesburg, South Africa, 6--12 June 2004), edited by D.L. Block & K. Freeman, Kluwer Academic Publisher, pp. 535--559

THE WARM, COLD AND VERY COLD DUSTY UNIVERSE

Aigen Li
Theoretical Astrophysics Program, University of Arizona, Tucson, AZ 85721

Abstract We are living in a dusty universe: dust is ubiquitously seen in a wide variety of astrophysical environments, ranging from circumstellar envelopes around cool red giants to supernova ejecta, from diffuse and dense interstellar clouds and star-forming regions to debris disks around main-sequence stars, from comets to interplanetary space to distant galaxies and quasars.

These grains, spanning a wide range of sizes from a few angstroms to a few micrometers, play a vital role in the evolution of galaxies as an absorber, scatterer, and emitter of electromagnetic radiation, as a driver for the mass loss of evolved stars, as an essential participant in the star and planet formation process, as an efficient catalyst for the formation of H_2 and other simple molecules as well as complex organic molecules which may lead to the origins of life, as a photoelectric heating agent for the interstellar gas, and as an agent shaping the spectral appearance of dusty systems such as protostars, young stellar objects, evolved stars and galaxies.

In this review I focus on the dust grains in the space between stars (interstellar dust), with particular emphasis on the extinction (absorption plus scattering) and emission properties of *cold* submicron-sized "classical" grains which, in thermal equilibrium with the ambient interstellar radiation field, obtain a steady-state temperature of $\sim$ 15–25 K, *warm* nano-sized (or smaller) "ultrasmall" grains which are, upon absorption of an energetic photon, transiently heated to temperatures as high as a few hundred to over 1000 K, and the possible existence of a population of *very cold* ($<$10 K) dust. Whether dust grains can really get down to "temperature" less than the 2.7 K cosmic microwave background radiation temperature will also be discussed. The robustness of the silicate-graphite-PAHs interstellar dust model is demonstrated by showing that the infrared emission predicted from this model closely matches that observed for the Milky Way, the Small Magellanic Cloud, and the ringed Sb galaxy NGC 7331.

Keywords: Interstellar dust – extinction – absorption – infrared emission

1. Introduction

The space between the stars (interstellar space) of the Milky Way Galaxy and other galaxies is filled with gaseous ions, atoms, molecules (interstellar gas) and tiny dust grains (interstellar dust). The first direct evidence which pointed to the existence of interstellar gas came from the ground-based detection of Na and Ca^+ optical absorption lines (Hartmann 1904).[1] This did not gain wide acceptance until Struve (1929) showed that the strength of the

Ca^+ K-line was correlated with the distance of the star. The true interstellar nature of this gas was further supported by the detection of the first interstellar molecules CH, CH^+ and CN (Swings & Rosenfeld 1937, McKellar 1940, Douglas & Herzberg 1941). The presence of dark, obscuring matter in the Milky Way Galaxy was also recognized at the beginning of the 20th century (e.g. see Barnard 1919). Trumpler (1930) first convincingly showed that this "obscuring matter" which dims and reddens starlight consists of small solid dust grains. The dust and gas are generally well mixed in the interstellar medium (ISM), as demonstrated observationally by the reasonably uniform correlation in the diffuse ISM between the hydrogen column density $N_{\rm H}$ and the dust extinction color excess or reddening $E(B-V) \equiv A_B - A_V$: $N_{\rm H}/E(B-V) \approx 5.8 \times 10^{21}\,{\rm mag}^{-1}\,{\rm cm}^{-2}$ (Bohlin et al. 1978), where A_B and A_V are the extinction at the B ($\lambda = 4400$ Å) and V ($\lambda = 5500$ Å) wavelength bands. From this correlation one can estimate the gas-to-dust ratio to be ~ 210 in the diffuse ISM.[2] Despite its tiny contribution to the total mass of a galaxy,[3] interstellar dust has a dramatic effect on the physical conditions and processes taking place within the universe, in particular, the evolution of galaxies and the formation of stars and planetary systems (see the introduction section of Li & Greenberg 2003).

In this review I will concentrate on the radiative properties of interstellar dust. I will distinguish the dust in terms of 3 components: **cold dust** with steady-state temperatures of $15\,{\rm K} \lesssim T \lesssim 25\,{\rm K}$ in thermal equilibrium with the solar neighbourhood interstellar radiation field, **very cold dust** with $T < 10\,{\rm K}$ (typically $T \sim 5\,{\rm K}$), and **warm dust** undergoing "temperature spikes" via single-photon heating. I will first summarize in §2 the observational constraints on the physical and chemical properties of interstellar dust. I will then discuss in §3 the heating and cooling properties of the warm and cold interstellar dust components. In §4 I will demonstrate the robustness of the silicate-graphite-PAHs interstellar grain model by showing that this model closely reproduces the observed infrared (IR) emission of the Milky Way, the Small Magellanic Cloud, and the ringed Sb galaxy NGC 7331. The possible existence of a population of very cold dust (with $T < 10\,{\rm K}$) in interstellar space will be discussed in §5. Whether ultrasmall grains can really cool down to $T < 2.7\,{\rm K}$ and appear in absorption against the cosmic microwave background (CMB) radiation will be discussed in §6.

2. Observational Constraints on Interstellar Dust

Our knowledge of interstellar dust regarding its composition, size and shape is mainly derived from its interaction with electromagnetic radiation: attenuation (absorption and scattering) and polarization of starlight, and emission of IR and far-IR radiation. The principal observational keys, both direct and indirect, used to constrain the properties of dust are the following:

- **(1) Interstellar Extinction.** Extinction is a combined effect of absorption and scattering: a grain in the line of sight between a distant star and the observer reduces the starlight by a combination of scattering and absorption (the absorbed energy is then re-radiated in the IR and far-IR).
  - The wavelength dependence of interstellar extinction – "interstellar extinction curve", most commonly determined from the "pair-method",[4] rise from the near-IR to the near-UV, with a broad absorption feature at about $\lambda^{-1}\approx 4.6\,\mu\mathrm{m}^{-1}$ ($\lambda\approx 2175$ A), followed by a steep rise into the far-UV $\lambda^{-1}\approx 10\,\mu\mathrm{m}^{-1}$. $\longrightarrow$ **The extinction curve tells us the size (and to a less extent, the composition) of interstellar dust.** Since it is generally true that a grain absorbs and scatters light most effectively at wavelengths comparable to its size $\lambda\approx 2\pi a$ (Krügel 2003), there must exist in the ISM a population of large grains with $a\gtrsim\lambda/2\pi\approx 0.1\,\mu\mathrm{m}$ to account for the extinction at visible wavelengths, and a population of ultrasmall grains with $a\lesssim\lambda/2\pi\approx 0.016\,\mu\mathrm{m}$ to account for the far-UV extinction at λ=0.1 μm (see Li 2004a for details).
  - The optical/UV extinction curves show considerable regional variations. $\longrightarrow$ **Dust grains on different sightlines have different size distributions (and/or different compositions).**
  - The optical/UV extinction curve in the wavelength range of $0.125\leq\lambda\leq 3.5\,\mu\mathrm{m}$ can be approximated by an analytical formula involving only one free parameter: $R_V\equiv A_V/E(B-V)$, the total-to-selective extinction ratio (Cardelli, Clayton, & Mathis 1989), whereas the near-IR extinction curve ($0.9\,\mu\mathrm{m}\leq\lambda\leq 3.5\,\mu\mathrm{m}$) can be fitted reasonably well by a power law $A(\lambda)\sim\lambda^{-1.7}$, showing little environmental variations.

    The Galactic mean extinction curve is characterized by $R_V\approx 3.1$. Values of R_V as small as 2.1 (the high latitude translucent molecular cloud HD 210121; Larson, Whittet, & Hough 1996; Li & Greenberg 1998) and as large as 5.6 (the HD 36982 molecular cloud in the Orion nebula) have been observed in the Galactic regions. More extreme extinction curves have been reported for extragalactic objects.[5] $\longrightarrow$ **The optical/UV extinction curve and the value of R_V depend on the environment**: lower-density regions have a smaller R_V, a stronger 2175 A hump and a steeper far-UV rise ($\lambda^{-1}>4\,\mu\mathrm{m}^{-1}$), implying smaller grains in these regions; denser regions have a larger R_V, a weaker 2175 A hump and a flatter far-UV rise, implying larger grains.
  - In the Small Magellanic Cloud (SMC), the extinction curves of most sightlines display a nearly linear steep rise with λ^{-1} and

an extremely weak or absent 2175 Å hump (Lequeux et al. 1982; Prévot et al. 1984). $\longrightarrow$ **Grains in the SMC are smaller than those in the Milky Way diffuse ISM as a result of either more efficient dust destruction in the SMC due to its harsh environment of the copious star formation associated with the SMC Bar or lack of growth due to the low-metallicity of the SMC, or both.** Regional variations also exist in the SMC extinction curves.[6]

- The Large Magellanic Cloud (LMC) extinction curve is characterized by a weaker 2175 Å hump and a stronger far-UV rise than the average Galactic extinction curve (Nandy et al. 1981; Koornneef & Code 1981).[7]

- **(2) Interstellar Polarization.** For a non-spherical grain, the light of distant stars is polarized as a result of differential extinction for different alignments of the electric vector of the radiation.
  - The interstellar polarization curve rises from the IR, has a maximum somewhere in the optical and then decreases toward the UV. $\longrightarrow$ **This tells us that (1) some fraction of interstellar grains are both non-spherical and aligned by some process; (2) the bulk of the aligned grains responsible for the peak polarization (at $\lambda\approx$0.55 μm) have typical sizes of $a\approx\lambda/2\pi\approx$0.1 μm; and (3) the ultrasmall grain component responsible for the far-UV extinction rise is either spherical or not aligned.**
  - The optical/UV polarization curve $P(\lambda)$ can be closely approximated by the "Serkowski law", an empirical function: $P(\lambda)/P_{\rm max} = \exp[-K\ln^2(\lambda/\lambda_{\rm max})]$, where the only one free parameter, $\lambda_{\rm max}$, is the wavelength where the maximum polarization $P_{\rm max}$ occurs, and K is the width parameter: $K\approx1.66\lambda_{\rm max}+0.01$; $\lambda_{\rm max}$ is indicative of grain size and correlated with R_V: $R_V \approx (5.6\pm0.3)\lambda_{\rm max}$ ($\lambda_{\rm max}$ is in micron; see Whittet 2003). $\longrightarrow$ **The sightlines with larger $\lambda_{\rm max}$ are rich in larger grains and have larger R_V for their extinction curves.** A close correlation between $\lambda_{\rm max}$ and the size of the aligned grains [e.g., $\lambda_{\rm max}\approx2\pi a(n-1)$ for dielectric cylinders of radius a and refractive index n] is predicted by interstellar extinction calculations.
  - The near-IR ($1.64\,\mu{\rm m}<\lambda<5\,\mu{\rm m}$) polarization is better approximated by a power law $P(\lambda)\propto\lambda^{-\beta}$, with $\beta\simeq1.8\pm0.2$, independent of $\lambda_{\rm max}$ (Martin & Whittet 1990, Martin et al. 1992).

- **(3) Interstellar Scattering.** Scattering of starlight by interstellar dust is revealed by reflection nebulae (dense clouds illuminated by embedded or nearby bright stars), dark clouds (illuminated by the general interstellar radiation field [ISRF]), and the diffuse Galactic light ("DGL";

starlight scattered off the general diffuse ISM of the Milky Way Galaxy illuminated by the general ISRF). The scattering properties of dust grains (albedo = ratio of scattering to extinction, and phase function) provide a means of constraining the optical properties of the grains and are therefore indicators of their size and composition and provide diagnostic tests for dust models.

- The albedo in the near-IR and optical is quite high (~ 0.6), with a clear dip to ~ 0.4 around the 2175 Å hump, a rise to ~ 0.8 around $\lambda^{-1}{\approx}6.6\,\mu\mathrm{m}^{-1}$, and a drop to ~ 0.3 by $\lambda^{-1}{\approx}10\,\mu\mathrm{m}^{-1}$; the scattering asymmetry factor almost monotonically rises from ~ 0.6 to ~ 0.8 from $\lambda^{-1}{\approx}1\,\mu\mathrm{m}^{-1}$ to $\lambda^{-1}{\approx}10\,\mu\mathrm{m}^{-1}$ (see Gordon 2004). $\longrightarrow$ **An appreciable fraction of the extinction in the near-IR and optical must arise from scattering; the 2175 Å hump is an absorption feature with no scattered component (see §2.4); and ultrasmall grains are predominantly absorptive.**
- Surprisingly high near-IR albedo has been reported for several regions: ~ 0.86 at the K′ band ($\lambda{\approx}2.1\,\mu\mathrm{m}$) for the prominent dust lane in the evil eye galaxy NGC 4826 (Witt et al. 1994), ~ 0.9 at the K′ band for the dust in the M 51 arm (Block 1996), and ~ 0.7 at the J ($\lambda{\approx}1.26\,\mu\mathrm{m}$) and H ($\lambda{\approx}1.66\,\mu\mathrm{m}$) bands and ~ 0.6 at the K ($\lambda{\approx}2.16\,\mu\mathrm{m}$) band for the Thumbprint Nebula (Lehtinen & Mattila 1996), in comparison with ~ 0.2 at λ=2.2 μm predicted by the conventional dust models (Draine & Lee 1984; Li & Greenberg 1997). $\longrightarrow$ This implies that for NGC 4826 and M 51 (1) a population of grains at least $\sim 0.5\,\mu\mathrm{m}$ in radii, twice as large as assumed by standard models, may exist in these environments and are responsible for the near-IR scattering; and/or (2) the measured high K′ surface-brightness and the deduced high albedo may in part be caused by the thermal continuum emission from stochastically heated ultrasmall grains (Witt et al. 1994; Block 1996). For the Thumbprint Nebula, the high near-IR albedo is readily explained by grain growth (larger-than-average grain sizes) and the accretion of an ice mantle (see Pendleton, Tielens, & Werner 1990; §8 in Li & Greenberg 1997).
- Scatterings of X-rays by interstellar dust have also been observed as evidenced by "X-ray halos" formed around an X-ray point source by small-angle scattering. The intensity and radial profile of the halo depends on the composition, size and morphology and the spatial distribution of the scattering dust particles (see Dwek et al. 2004 for a review). The total and differential cross sections for X-ray scattering approximately vary as a^4 and a^6, respectively, **the shape and intensity of X-ray halos surrounding X-ray point**

sources therefore provide one of the most sensitive constraints on the largest grains along the sightline, while these grains are gray at optical wavelengths and therefore the near-IR to far-UV extinction modeling is unable to constrain their existence.

A recent study of the X-ray halo around Nova Cygni 1992 by Witt, Smith, & Dwek (2001) pointed to the requirement of large interstellar grains ($a \sim 0.25$–$2\,\mu$m), consistent with the recent Ulysses and Galileo detections of interstellar dust entering our solar system (Grün et al. 1994; Frisch et al. 1999; Landgraf et al. 2000). But Draine & Tan (2003) found that the silicate-graphite-PAH model with the dust size distributions derived from the near-IR to far-UV extinction modeling (Weingartner & Draine 2001a) and IR emission modeling (Li & Draine 2001b) is able to explain the observed X-ray halo.

- **(4) Spectroscopic Extinction and Polarization Features: <u>The 2175 Å Extinction Hump</u> – the strongest spectroscopic extinction feature.**
  - Its strength and width vary with environment while its peak position is quite invariant: the central wavelength of this feature varies by only $\pm 0.46\%$ (2σ) around 2175 Å ($4.6\,\mu\mathrm{m}^{-1}$), while its FWHM varies by $\pm 12\%$ (2σ) around 469 Å ($\approx 1\,\mu\mathrm{m}^{-1}$).
  - Its carrier remains unidentified 39 years after its first detection (Stecher 1965). It is generally believed to be caused by aromatic carbonaceous (graphitic) materials, very likely a cosmic mixture of polycyclic aromatic hydrocarbon (PAH) molecules (Joblin, Léger & Martin 1992; Li & Draine 2001b; Draine 2003a).
  - For most sightlines, this feature is unpolarized. So far only two lines of sight toward HD 147933 and HD 197770 have a weak 2175 Å polarization feature detected (Clayton et al. 1992; Anderson et al. 1996; Wolff et al. 1997; Martin, Clayton, & Wolff 1999). Even for these sightlines, the degree of alignment and/or polarizing ability of the carrier should be very small (see Li & Greenberg 2003).
  - Except for the detection of scattering in the 2175 Å hump in two reflection nebulae (Witt, Bohlin, & Stecher 1986), the 2175 Å hump is thought to be predominantly due to absorption, suggesting its carrier is sufficiently small to be in the Rayleigh limit.
  - The detections of this feature in distant objects have been reported by Malhotra (1997) in the composite absorption spectrum of 96 intervening Mg II absorption systems at $0.2 < z < 2.2$; by Cohen et al. (1999) in a damped Lyα absorber (DLA) at $z = 0.94$; by Toft, Hjorth & Burud (2000) in a lensing galaxy at $z = 0.44$; by Motta

et al. (2002) in a lensing galaxy at $z = 0.83$; and very recently by Wang et al. (2004) in 3 intervening quasar absorption systems at $1.4 \lesssim z \lesssim 1.5$.

- **(5) Spectroscopic Extinction and Polarization Features: The 9.7 μm and 18 μm (Silicate) Absorption Features – the strongest IR Absorption features.**
  - Ubiquitously seen in a wide range of astrophysical environments, these features are almost certainly due to silicate minerals: they are respectively ascribed to the Si-O stretching and O-Si-O bending modes in some form of silicate material (e.g. olivine $Mg_{2x}Fe_{2-2x}SiO_4$).
  - The observed interstellar silicate bands are broad and relatively featureless. $\longrightarrow$ **Interstellar silicates are largely amorphous rather than crystalline.** Li & Draine (2001a) estimated that the amount of $a<1\,\mu$m crystalline silicate grains in the diffuse ISM is $<5\%$ of the solar Si abundance.[8]
  - The strength of the $9.7\,\mu$m feature is approximately $\Delta\tau_{9.7\,\mu m}/A_V \approx 1/18.5$ in the local diffuse ISM. $\longrightarrow$ **Almost all Si atoms have been locked up in silicate dust, if assuming solar abundance for the ISM.**[9]
  - The 9.7 and $18\,\mu$m silicate absorption features are polarized in some interstellar regions, most of which are featureless. The only exception is AFGL 2591, a molecular cloud surrounding a young stellar object, which displays a narrow feature at $11.2\,\mu$m superimposed on the broad $9.7\,\mu$m polarization band, generally attributed to annealed silicates (Aitken et al. 1988).

- **(6) Spectroscopic Extinction and Polarization Features: The 3.4 μm (Aliphatic Hydrocarbon) Absorption Feature.**
  - Widely seen in the diffuse ISM of the Milky Way Galaxy and other galaxies (e.g. Seyfert galaxies and ultraluminous infrared galaxies, see Pendleton 2004 for a recent review), this strong absorption band is attributed to the C-H stretching mode in **aliphatic hydrocarbon dust**. Its exact nature remains uncertain, despite 23 years' extensive investigation with over 20 different candidates proposed (see Pendleton & Allamandola 2002 for a summary). So far, the experimental spectra of hydrogenated amorphous carbon (HAC; Schnaiter, Henning & Mutschke 1999, Mennella et al. 1999) and the organic refractory residue, synthesized from UV photoprocessing of interstellar ice mixtures (Greenberg et al. 1995), provide the best fit to both the overall feature and the positions and relative

strengths of the 3.42 μm, 3.48 μm, and 3.51 μm subfeatures corresponding to symmetric and asymmetric stretches of C–H bonds in CH_2 and CH_3 groups. Pendleton & Allamandola (2002) attributed this feature to hydrocarbons with a mixed aromatic and aliphatic character.

- The 3.4 μm band strength for interstellar aliphatic hydrocarbon dust is unknown. If we adopt a mass absorption coefficient of $\kappa_{\rm abs}(3.4\,\mu{\rm m}) \sim 1500\,{\rm cm^2\,g^{-1}}$ (Li & Greenberg 2002), we would require $\sim$68 ppm C to be locked up in this dust component to account for the local ISM 3.4 μm feature ($\Delta\tau_{3.4\,\mu{\rm m}}/A_V \approx 1/250$; Pendleton et al. 1994).
- **This feature is ubiquitously seen in the diffuse ISM while never detected in molecular clouds**. Mennella et al. (2001) and Muñoz Caro et al. (2001) argue that this can be explained by the competition between dehydrogenation (destruction of C-H bonds by UV photons) and rehydrogenation (formation of C-H bonds by H atoms interacting with the carbon dust): in diffuse clouds, rehydrogenation prevails over dehydrogenation; in dense molecular clouds, dehydrogenation prevails over rehydrogenation as a result of the reduced amount of H atoms and the presence of ice mantles which inhibits the hydrogenation of the underlying carbon dust by H atoms while dehydrogenation can still proceed since the UV radiation can penetrate the ice layers.
- Whether the origin of the interstellar aliphatic hydrocarbon dust occurs in the outflow of carbon stars or in the ISM itself is a subject of debate. The former gains strength from the close similarity between the 3.4 μm interstellar feature and that of a carbon-rich protoplanetary nebula CRL 618 (Lequeux & Jourdain de Muizon 1990; Chiar et al. 1998). However, the survival of the stellar-origin dust in the diffuse ISM is questionable (see Draine 1990).
- So far, **no polarization has been detected for this feature** (Adamson et al. 1999).[10] Spectropolarimetric measurements for both the 9.7 μm silicate and the 3.4 μm hydrocarbon features for the same sightline would allow a direct test of the silicate core-hydrocarbon mantle interstellar dust model (Li & Greenberg 1997), since this model predicts that the 3.4 μm feature would be polarized if the 9.7 μm feature (for the same sightline) is polarized (Li & Greenberg 2002).

- **(7) Spectroscopic Extinction and Polarization Features: <u>The Ice Absorption Features.</u>**

- Grains in dark molecular clouds (usually with $A_V > 3$ mag) obtain ice mantles consisting of H_2O, NH_3, CO, CH_3OH, CO_2, CH_4, H_2CO and other molecules (with H_2O as the dominant species), as revealed by the detection of various ice absorption features (e.g., H_2O: 3.1, 6.0 μm; CO: 4.67 μm; CO_2: 4.27, 15.2 μm; CH_3OH: 3.54, 9.75 μm; NH_3: 2.97 μm; CH_4: 7.68 μm; H_2CO: 5.81 μm; OCN^-: 4.62 μm; see Boogert & Ehrenfreund 2004 for a review).
- Polarization has been detected in the 3.1 μm H_2O, the 4.67 μm CO and 4.62 μm OCN^- absorption features (e.g. see Chrysostomou et al. 1996).

- **(8) The Extended Red Emission: Dust Photoluminescence.** The "Extended Red Emission" (ERE), widely seen in reflection nebulae, planetary nebulae, HII regions, the Milky Way diffuse ISM, and other galaxies, is a far-red continuum emission in excess of what is expected from simple scattering of starlight by interstellar dust (see Witt & Vijh 2004). The ERE is characterized by a broad, featureless band between $\sim$ 5400 A and 9500 A, with a width $600\,\mathrm{A} \lesssim \mathrm{FWHM} \lesssim 1000\,\mathrm{A}$ and a peak of maximum emission at $6100\,\mathrm{A} \lesssim \lambda_\mathrm{p} \lesssim 8200\,\mathrm{A}$, depending on the physical conditions of the environment where the ERE is produced.
  - The ERE is generally attributed to photoluminescence (PL) by some component of interstellar dust, powered by UV/visible photons with a photon conversion efficiency $\eta_\mathrm{PL} \gg 10\%$ (Gordon, Witt, & Friedmann 1998). $\longrightarrow$ **The ERE carriers are very likely in the nanometer size range** because nanoparticles are expected to luminesce efficiently through the recombination of the electron-hole pair created upon absorption of an energetic photon, since in such small systems the excited electron is spatially confined and the radiationless transitions that are facilitated by Auger and defect related recombination are reduced (see Li 2004a).
  - The ERE carrier remains unidentified. Various candidate materials have been proposed, but most of them appear unable to match the observed ERE spectra and satisfy the high-η_PL requirement (Draine 2003a; Li & Draine 2002a; Li 2004a; Witt & Vijh 2004). Promising candidates include PAHs (d'Hendecourt et al. 1986) and silicon nanoparticles (Ledoux et al. 1998, Witt et al. 1998, Smith & Witt 2002), but both have their own problems (see Li & Draine 2002a).

- **(9) Spectroscopic Emission Features: The 3.3, 6.2, 7.7, 8.6, 11.3 μm "Unidentified Infrared (UIR) Emission features.** The distinctive set of "UIR" emission features at 3.3, 6.2, 7.7, 8.6, and 11.3 μm are seen in

a wide variety of objects, including planetary nebulae, protoplanetary nebulae, reflection nebulae, HII regions, photodissociation fronts, circumstellar envelopes, and external galaxies.

- **These "UIR" emission features are now generally identified as vibrational modes of PAHs** (Léger & Puget 1984; Allamandola, Tielens, & Barker 1985): C–H stretching mode (3.3 μm), C–C stretching modes (6.2 and 7.7 μm), C–H in-plane bending mode (8.6 μm), and C–H out-of-plane bending mode (11.3 μm).[11] **The relative strengths and precise wavelengths of these features are dependent on the PAH size and its ionization state** which is controlled by the starlight intensity, electron density, and gas temperature of the environment (Bakes & Tielens 1994, Weingartner & Draine 2001b, Draine & Li 2001).
- **Stochastically heated by the absorption of a single UV/visible photon (Draine & Li 2001; Li 2004a), PAHs, containing $\sim$ 45 ppm C, account for $\sim$ 20% of the total power emitted by interstellar dust in the Milky Way diffuse ISM (Li & Draine 2001b).**
- **The excitation of PAHs does not require UV photons;** long wavelength (red and far-red) photons are also able to heat PAHs to high temperatures so that they emit efficiently at the UIR bands. This is because **the PAH electronic absorption edge shifts to longer wavelengths upon ionization and/or as the PAH size increases**.[12]
- No polarization has been detected for the PAH emission features (Sellgren, Rouan, & Léger 1988).
- The **PAH absorption features** at 3.3 μm and 6.2 μm have been detected in both local sources and Galactic Center sources (Schutte et al. 1998; Chiar et al. 2000). The strengths of these features are in good agreement with those predicted from the astronomical PAH model (Li & Draine 2001b).
- **PAHs can be rotationally excited** by a number of physical processes, including collisions with neutral atoms and ions, "plasma drag", and absorption and emission of photons. It is shown that these processes can drive PAHs to rapidly rotate, with rotation rates reaching tens of GHz. The rotational electric dipole emission from these spinning PAH molecules is capable of accounting for the observed "anomalous" microwave emission (Draine & Lazarian 1998a,b; Draine 1999; Draine & Li 2004).

■ **(10) <u>IR Emission from Interstellar Dust.</u>** Interstellar grains absorb starlight in the UV/visible and re-radiate in the IR. The IR emission spectrum of the Milky Way diffuse ISM, estimated using the IRAS 12, 25, 60

and 100 μm broadband photometry, the DIRBE-COBE 2.2, 3.5, 4.9, 12, 25, 60, 100, 140 and 240 μm broadband photometry, and the FIRAS-COBE 110 μm$<\lambda<$3000 μm spectrophotometry, is characterized by a modified black-body of $\lambda^{-1.7}B_\lambda$(T=19.5 K) peaking at $\sim$ 130 μm in the wavelength range of 80 μm$\lesssim\lambda\lesssim$1000 μm, and a substantial amount of emission at $\lambda\lesssim$60 μm which far exceeds what would be expected from dust at $T\approx$20 K (see Draine 2003a). In addition, spectrometers aboard the IRTS (Onaka et al. 1996; Tanaka et al. 1996) and ISO (Mattila et al. 1996) have shown that the diffuse ISM radiates strongly in emission features at 3.3, 6.2, 7.7, 8.6, and 11.3 μm.

- The emission at $\lambda\gtrsim$60 μm accounts for $\sim$ 65% of the total emitted power. $\longrightarrow$ There must exist a population of **"cold dust"** in the size range of $a>$250 A, heated by starlight to equilibrium temperatures 15 K$\lesssim T\lesssim$25 K and cooled by far-IR emission (see Li & Draine 2001b).
- The emission at $\lambda\lesssim$60 μm accounts for $\sim$ 35% of the total emitted power. $\longrightarrow$ There must exist a population of **"warm dust"** in the size range of $a<$250 A, stochastically heated by single starlight photons to temperatures $T\gg$20 K and cooled by near- and mid-IR emission (see Li & Draine 2001b; Li 2004a).

- **(11) Interstellar Depletions.** Atoms locked up in dust grains are "depleted" from the gas phase. The dust depletion can be determined from comparing the gas-phase abundances measured from optical and UV absorption spectroscopic lines with the assumed reference abundances of the ISM (total abundances of atoms both in gas and in dust; also known as "standard abundances", "interstellar abundances", and "cosmic abundances"). The total interstellar abundances are usually taken to be solar, although Snow & Witt (1996) argued that interstellar abundances are appreciably subsolar ($\sim$ 70% solar). Interstellar depletions allow us to extract important information about the composition and quantity of interstellar dust:
  - In low density clouds, Si, Fe, Mg, C, and O are depleted. $\longrightarrow$ **Interstellar dust must contain an appreciable amount of Si, Fe, Mg, C and O.** Indeed, all contemporary interstellar dust models consist of both silicates and carbonaceous dust.
  - From the depletion of the major elements Si, Fe, Mg, C, and O one can estimate **the gas-to-dust mass ratio to be $\sim$ 165**.[13]
  - In addition to the silicate dust component, there must exist another dust population, since **silicates alone are not able to account for the observed amount of extinction relative to H** although Si, Mg,

and Fe are highly depleted in the ISM. Even if all Si, Fe, and Mg elements are locked up in submicron-sized silicate grains, they can only account for $\sim 60\%$ of the total observed optical extinction.[14]

3. Warm and Cold Dust in the ISM

As summarized in §2, the interstellar extinction, polarization, scattering, the near, mid, and far-IR emission and the 3.3–11.3 μm PAH emission features point to the existence of two dust populations in interstellar space:

- There exists a population of large grains with $a \gtrsim 250\,\mathrm{A}$. Illuminated by the general interstellar radiation field (ISRF), these grains, defined as **"cold dust"**, obtain equilibrium temperatures of $15\,\mathrm{K} \lesssim T \lesssim 25\,\mathrm{K}$ and emit strongly at wavelengths $\lambda \gtrsim 60\,\mu\mathrm{m}$. These grains are responsible for the near-IR/optical extinction, scattering, polarization and the emission at $\lambda \gtrsim 60\,\mu\mathrm{m}$.

  The equilibrium temperature T for a large grain of spherical radius a is determined by balancing absorption and emission:

$$\int_0^\infty C_{\rm abs}(a,\lambda) c u_\lambda d\lambda = \int_0^\infty C_{\rm abs}(a,\lambda) 4\pi B_\lambda(T) d\lambda \ , \qquad (1)$$

  where $C_{\rm abs}(a,\lambda)$ is the absorption cross section for a grain with size a at wavelength λ, c is the speed of light, $B_\lambda(T)$ is the Planck function at temperature T, and u_λ is the energy density of the radiation field. In Figure 1 we display these "equilibrium" temperatures for graphitic and silicate grains as a function of size in environments with various UV intensities.

- There exists a population of ultrasmall grains with $a \lesssim 250\,\mathrm{A}$. These grains have energy contents smaller or comparable to the energy of a single starlight photon. As a result, a single photon can heat a very small grain to a peak temperature much higher than its "steady-state" temperature and the grain then rapidly cools down to a temperature below the "steady-state" temperature before the next photon absorption event. Stochastic heating by absorption of starlight therefore results in transient "temperature spikes", during which much of the energy deposited by the starlight photon is reradiated in the IR – because of this, we call these ultrasmall grains **"warm dust"**.[15] These grains are responsible for the far-UV extinction rise and the emission at $\lambda \lesssim 60\,\mu\mathrm{m}$ (including the 3.3–11.3 μm PAH emission features), dominate the photoelectric heating of interstellar gas (see §2.5 in Li 2004a), and provide most of the grain surface area in the diffuse ISM.

  Since ultrasmall grains will not maintain "equilibrium temperatures", we need to calculate their temperature (energy) probability distribution

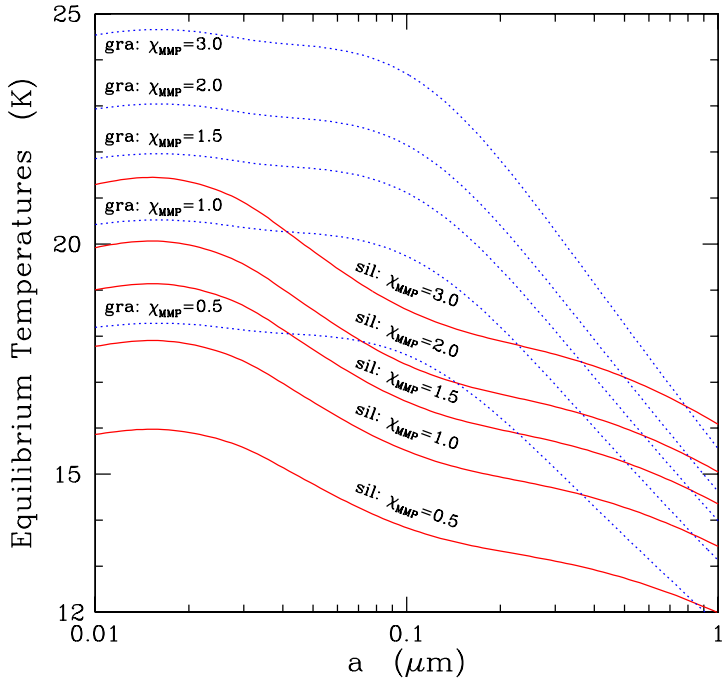

Figure 1. Equilibrium temperatures for graphite (dotted lines) and silicate grains (solid lines) in environments with various starlight intensities (in units of the Mathis, Mezger, & Panagia 1983 [MMP] solar neighbourhood ISRF). Taken from Li & Draine (2001b).

functions in order to calculate their time-averaged IR emission spectrum. There have been a number of studies on this topic since the pioneering work of Greenberg (1968). A recent extensive investigation was carried out by Draine & Li (2001). We will not go into details in this review, but just refer those who are interested to Draine & Li (2001) and a recent review article of Li (2004a).

For illustration, we show in Figure 2 the energy probability distribution functions $dP/d\ln E$ (where dP is the probability that a grain will have vibrational energy in interval $[E, E+dE]$) for PAHs with radii $a = 5, 10, 25, 50, 75, 100, 150, 200, 300$A illuminated by the general ISRF. It is seen that very small grains ($a \lesssim 100\,\mathrm{A}$) have a very broad $P(E)$, and the smallest grains ($a < 30\,\mathrm{A}$) have an appreciable probability P_0 of being found in the vibrational ground state E=0. As the grain size increases, $P(E)$ becomes narrower, so that it can be approximated by a delta function for $a > 250\,\mathrm{A}$.[16] However, for radii as large as a=200 A, grains have energy distribution functions which are broad enough that the emission spectrum deviates noticeably from the emission spectrum for grains at a single "steady-state" temperature T, as shown in Fig-

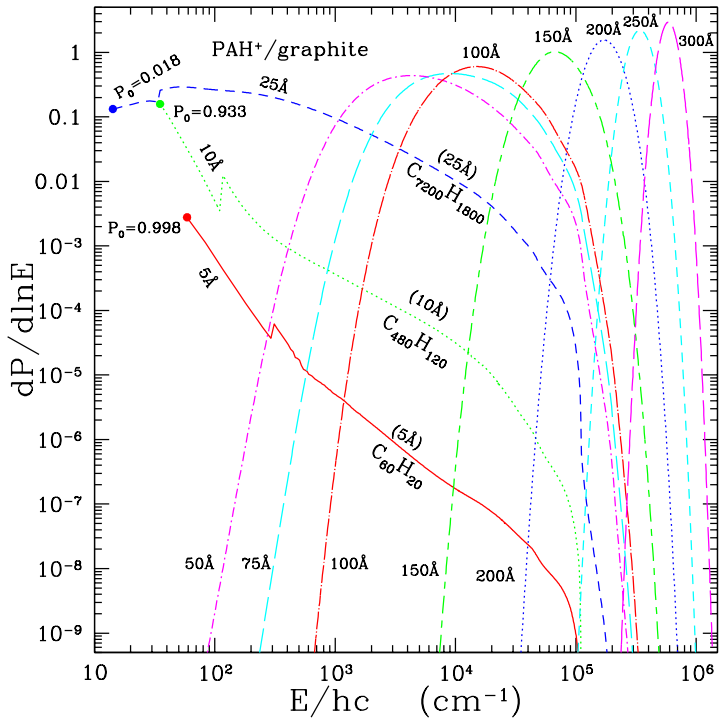

Figure 2. The energy probability distribution functions for charged carbonaceous grains (a = 5 Å [$C_{60}H_{20}$], 10 Å [$C_{480}H_{120}$], 25 Å [$C_{7200}H_{1800}$], 50, 75, 100, 150, 200, 250, 300 Å) illuminated by the general ISRF. The discontinuity in the 5, 10, and 25 Å curves is due to the change of the estimate for grain vibrational "temperature" at the 20th vibrational mode (see Draine & Li 2001). For 5, 10, and 25Å a dot indicates the first excited state, and P_0 is the probability of being in the ground state. Taken from Li & Draine (2001b).

ure 3. For accurate computation of IR emission spectra it is therefore important to properly calculate the energy distribution function $P(E)$, including grain sizes which are large enough that the average thermal energy content exceeds a few eV.

- Nano-sized *interstellar* diamond and TiC grains have been identified in primitive meteorites based on isotopic anomaly analysis. Exposed to the general ISRF, these grains are subject to single-photon heating and should of course be classified as "warm dust". But we should note that they are not representative of the bulk interstellar dust (see §5.4 and §5.5 in Li 2004a). The carriers of the ERE (see §2.8) and the 2175 Å extinction hump (see §2.4) are also in the single-photon heating regime. Therefore, they can also be classified as "warm dust". As a matter of fact, the latter is attributed to PAHs (see §2.4). On the other hand, the Ulysses and Galileo spacecrafts have detected a substantial number of large interstellar grains with $a \gtrsim 1\,\mu$m (Grün et al. 1994), much higher

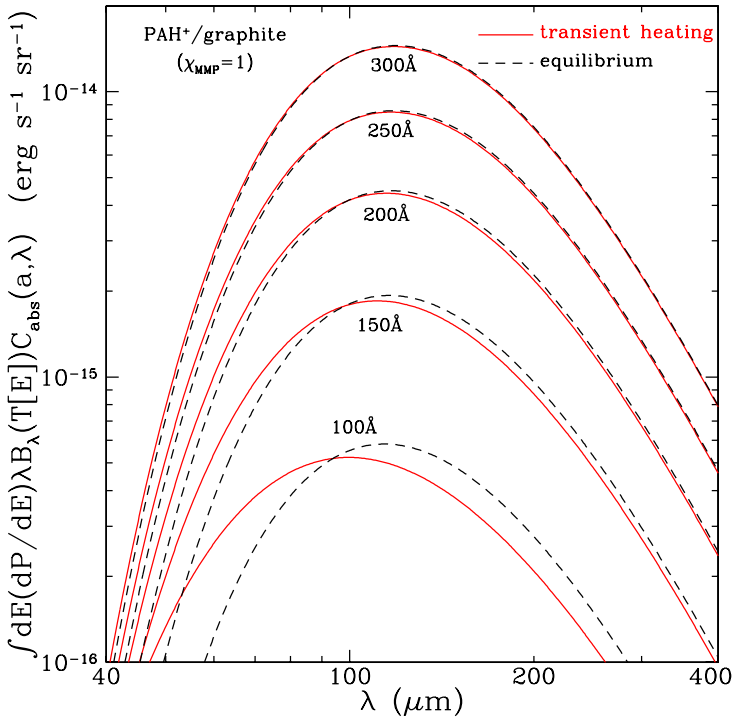

Figure 3. Infrared emission spectra for small carbonaceous grains of various sizes heated by the general ISRF, calculated using the full energy distribution function $P(E)$ (solid lines); also shown (broken lines) are spectra computed for grains at the "equilibrium" temperature T. Transient heating effects lead to signifi cantly more short wavelength emission for $a \lesssim 200$ A. Taken from Li & Draine (2001b).

than expected for the average interstellar dust distribution. In the ISM, these should of course be considered as "cold dust" or "very cold dust" with $T<10\,\mathrm{K}$. But we note that the reported mass of these large grains is diffi cult to reconcile with the interstellar extinction and interstellar elemental abundances.

4. The Silicate-Graphite-PAHs Interstellar Dust Model

Various models have been proposed for interstellar dust (see Li & Greenberg 2003, Li 2004a, Draine 2004 for recent reviews). In general, these models fall into three broad categories: the silicate core-carbonaceous mantle model (Li & Greenberg 1997), the silicate-graphite-PAHs model (Li & Draine 2001b, Weingartner & Draine 2001a) and the composite model (Mathis 1996, Zubko, Dwek & Arendt 2004). In this review I will focus on the IR emission calculated from the silicate-graphite-PAHs model and refer those who are interested in a detailed comparison between different models to my recent review articles (Li 2004a, Li & Greenberg 2003).

The silicate-graphite-PAHs model, consisting of a mixture of amorphous silicate dust and carbonaceous dust – each with an extended size distribution ranging from molecules containing tens of atoms to large grains $\gtrsim 1\,\mu$m in diameter, is a natural extension of the classical silicate-graphite model (Mathis, Rumpl, & Nordsieck 1977; Draine & Lee 1984). We assume that the carbonaceous grain population extends from grains with graphitic properties at radii $a \gtrsim 50$ Å, down to particles with PAH-like properties at very small sizes.

With the temperature (energy) probability distribution functions calculated for ultrasmall grains undergoing "temperature spikes" and equilibrium temperatures calculated for large grains illuminated by the local ISRF, the silicate-graphite-PAHs model with grain size distributions consistent with the observed R_V=3.1 interstellar extinction (Weingartner & Draine 2001a), is able to reproduce the observed near-IR to submillimeter emission spectrum of the diffuse ISM, including the PAH emission features at 3.3, 6.2, 7.7, 8.6, and 11.3 μm. This is demonstrated in Figure 4 and Figure 5 for the high-latitude "cirrus" cloud and 2 regions in the Galactic plane (see Li & Draine 2001b for details).

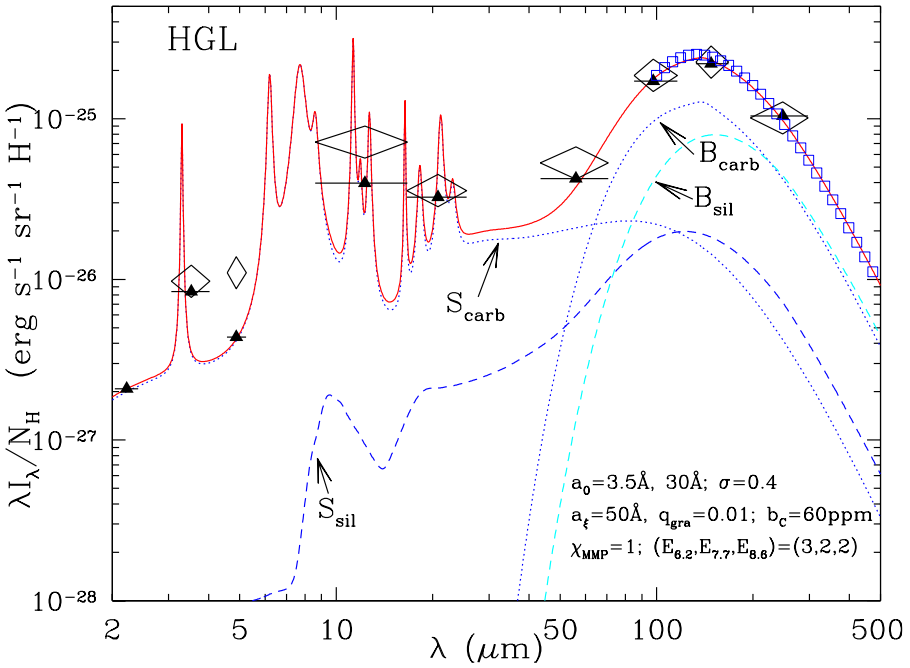

Figure 4. Comparison of the model to the observed emission from the diffuse ISM at high galactic latitudes ($|b| \geq 25^o$). Curves labelled B_{sil} and B_{carb} show emission from "big" ($a \geq 250$ A) silicate and carbonaceous grains; curves labelled S_{sil} and S_{carb} show emission from "small" ($a < 250$ A) silicate and carbonaceous grains (including PAHs). Triangles show the model spectrum (solid curve) convolved with the DIRBE filters. Observational data are from DIRBE (diamonds) and FIRAS (squares). Taken from Li & Draine (2001b).

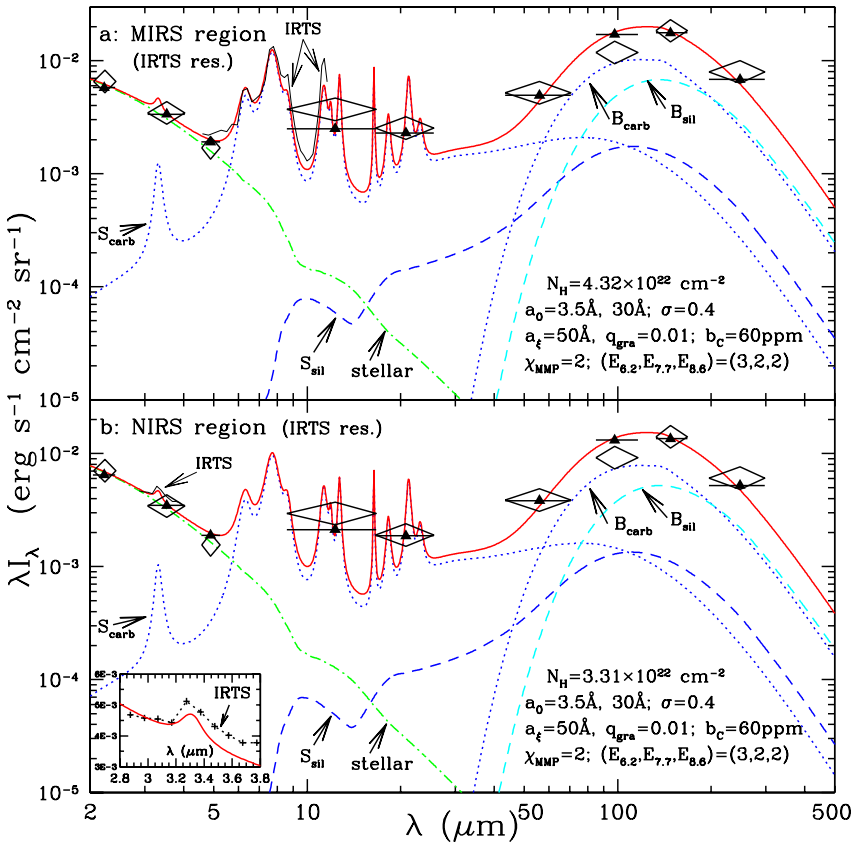

Figure 5. Infrared emission from dust plus starlight for two regions in the Galactic plane: (a) the MIRS region ($44° \leq l \leq 44°40', -0°40' \leq b \leq 0°$), and (b) the NIRS region ($47°30' \leq l \leq 48°$, $|b| \leq 15'$). The starlight intensity heating the dust has been taken to be twice the MMP ISRF. The solid curve shows the overall model spectrum; triangles show the model spectrum convolved with the DIRBE filters. DIRBE observations are shown as diamonds. For the MIRS field we show the IRTS MIRS 5–12 μm spectrum (thin solid line). For the NIRS field we show the IRTS NIRS 2.8-3.9 μm spectrum (thin solid line, also shown as cross-dotted curve in inset). Taken from Li & Draine (2001b).

The silicate-graphite-PAHs model, with size distributions consistent with the SMC Bar extinction curve (Weingartner & Draine 2001a), is also successful in reproducing the observed IR emission from the SMC (Li & Draine 2002c), as shown in Figure 6. The dust in the SMC is taken to be illuminated by a distribution of starlight intensities. Following Dale et al. (2001), we adopt a simple power-law function for the starlight intensity distribution. The SMC, with a low metallicity ($\sim 10\%$ of solar) and a low dust-to-gas ratio ($\sim 10\%$ of the Milky Way), has a very weak or no 2175 Å extinction hump in its extinction curves for most sightlines (see §2.1) and very weak 12 μm emission (see Fig. 6) which is generally attributed to PAHs, supporting the idea of PAHs as the carrier for the 2175 Å extinction hump.[17]

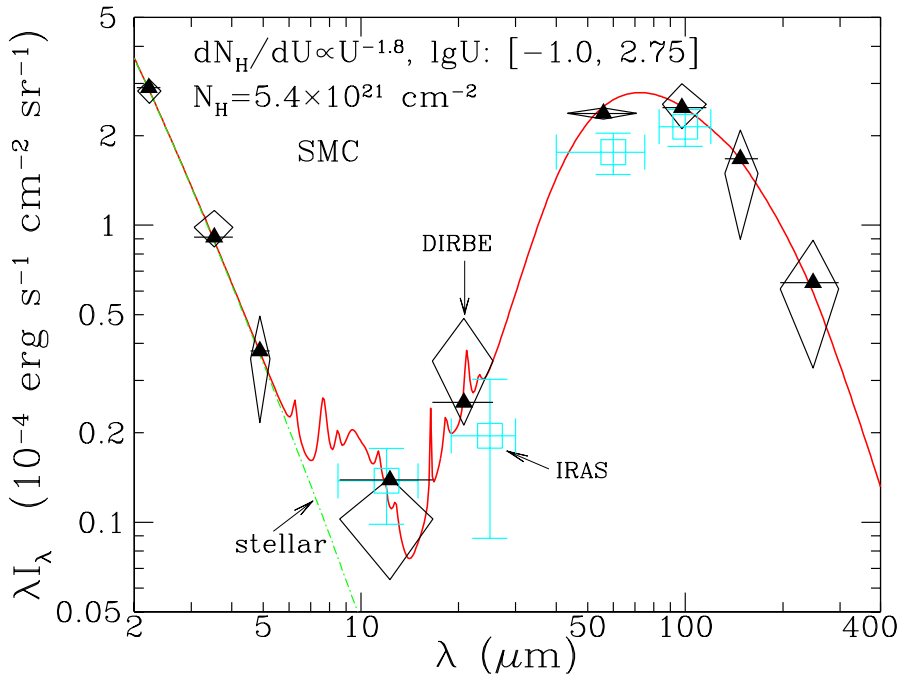

Figure 6. Comparison of the model (solid line) to the observed emission from the SMC obtained by COBE/DIRBE (diamonds) and IRAS (squares) averaged over a 6.25 deg^2 region including the optical bar and the Eastern Wing. Triangles show the model spectrum convolved with the DIRBE filters. Stellar radiation (dot-dashed line) dominates for $\lambda \lesssim 6\,\mu$m. Grains are illuminated by a range of radiation intensities $dN_{\rm H}/dU \propto U^{-1.8}$, $0.1 \leq U \leq 10^{2.75}$, with $N_{\rm H}^{\rm tot} \approx 5.4 \times 10^{21}$ cm^{-2}. Taken from Li & Draine (2002c).

Very recently, the silicate-graphite-PAHs model has also been successfully applied to NGC 7331, a ringed Sb galaxy. Using the same set of dust parameters determined for the Milky Way diffuse ISM (R_V=3.1; Weingartner & Draine 2001a), as shown in Figure 7, this model fits the IR emission observed by the IRAC instrument at 3.6, 4.5, 5.8 and 8 μm and the MIPS instrument at 24, 70 and 160 μm aboard the Spitzer Space Telescope and the 450 and 850 μm SCUBA submillimeter emission observed by JCMT, both for the ring and inside star-forming region and for the galaxy as whole (see Regan et al. 2004 for details). The model also closely reproduces the observed 6.2, 7.7, 8.6, 11.3 and 12.7 μm PAH emission features (see Fig. 2 of Smith et al. 2004).

5. Very Cold Dust or How Cold Could Galaxies Be?

In the 1996 South African "*Cold Dust*" Symposium (Block & Greenberg 1996), the possible existence of a population of **very cold dust** (with equilibrium temperatures $T<10$ K) in interstellar space was a subject received much attention. In his invited paper titled "*How Cold Could Galaxies Be?*" published in the proceedings for that symposium, Mike Disney wrote "... *An eminent cos-*

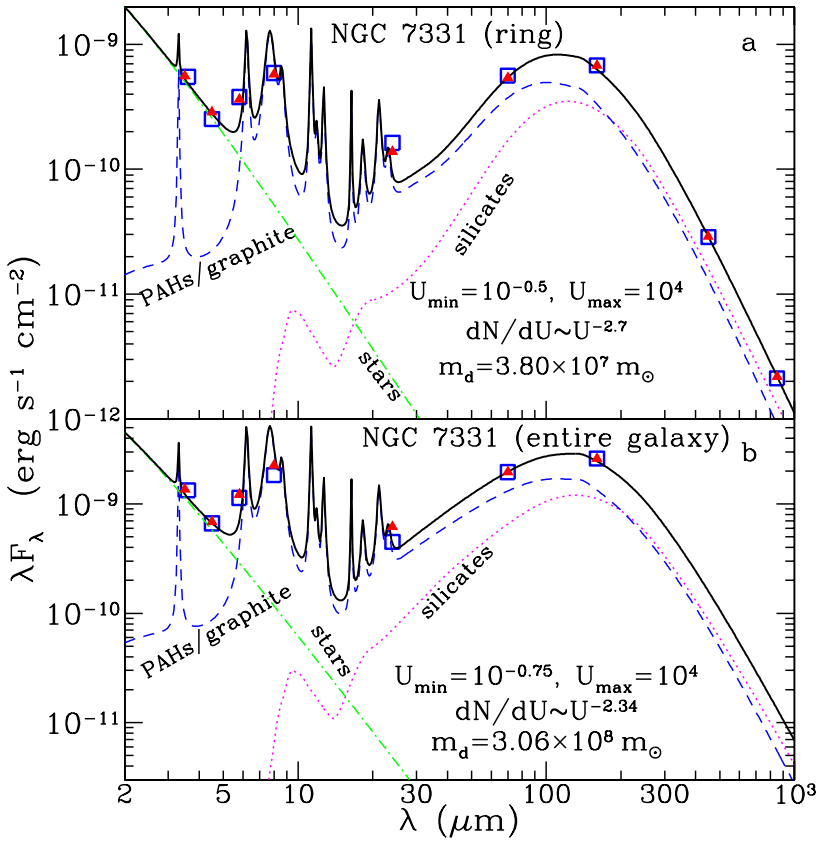

Figure 7. IR emission and model fits to the NGC 7331 ring (a) and the entire galaxy (b). The thick solid lines and triangles are the model-predicted fluxes, and the squares are the observed fluxes. The broken curves indicate the contributions of the different model components. Taken from Regan et al. (2004).

mologist once advised me to forget all about very cold dust because the T^4 law ensures that it cannot emit, and therefore by implication cannot absorb, much radiation. He sounded plausible, as Cosmologists are apt to sound, but he was in fact totally wrong, as Cosmologists are apt to be."

Disney (1996) argued that for grains with higher IR and far-IR emissivities, they can achieve rather low temperatures. At first glance, this appears plausible as can be seen in Eq.(1): for a given interstellar radiation field, grains with fixed UV and optical absorption properties would obtain lower temperatures if their long wavelength emissivities are enhanced. Therefore, Disney (1996) wrote "... *[Since] we are not confident about their [interstellar grains] size distribution and their emissivities, particularly at long wavelength, ...* **we have to keep our minds open to the possible existence of a significant amounts of very cold ($<10\,$K) material in spiral galaxies.**"

So far, the detection of very cold dust ($T<10\,\mathrm{K}$) in interstellar space on galactic scales has been reported for various objects: NGC 4631, a low metallicity ($\sim 1/2$ of solar) interacting galaxy with $T\sim 4$–$6\,\mathrm{K}$ (Dumke, Krause, & Wielebinski 2004); NGC 1569, a low metallicity ($\sim 1/4$ of solar) starbursting dwarf galaxy with $T\sim 5$–$7\,\mathrm{K}$ (Galliano et al. 2003); inactive spiral galaxies UGC 3490 with $T\sim 9\,\mathrm{K}$ (Chini et al. 1995), NGC 6156 with $T\sim 8.6\,\mathrm{K}$, and NGC 6918 with $T\sim 9.4\,\mathrm{K}$ (Krügel et al. 1998); and several irregular and blue compact dwarf galaxies with $T<10\,\mathrm{K}$ in the Virgo Cluster (Popescu et al. 2002). Very cold dust with $T\sim 4$–$7\,\mathrm{K}$ has also been detected in the Milky Way Galaxy (Reach et al. 1995; also see Boulanger et al. 2002). This component is widespread and spatially correlated with the warm component (16–21 K). By comparing the dust mass calculated from the IRAS data with the molecular and atomic gas masses of 58 spiral galaxies, Devereux & Young (1990) argued that the bulk of the dust in spiral galaxies is $<15\,\mathrm{K}$ regardless of the phase of the ISM.

How can dust get so cold? In literature, suggested solutions include (1) the dust is deeply embedded in clumpy clouds and heated by the far-IR emission from "classical grains" (Galliano et al. 2003; Dumke et al. 2004); [18] (2) the dust has unusual optical properties (e.g. fractal or porous grains with enhanced submm and mm emissivity; Reach et al. 1995; Dumke et al. 2004). **However, as discussed in detail by Li (2004b), while the former solution appears to be inconsistent with the fact that the very cold dust is observed on galactic scales, the latter violates the Kramers-Kronig dispersion relation (Purcell 1969; Draine 2003b; Li 2003b),** except for extremely elongated conducting dust (Li 2003a). Perhaps the submm and mm excess emission (usually attributed to very cold dust) is from something else? To avoid the "temperature" problem, one can adopt the Block direct method to identify and characterize the presence and distribution of the cold and very cold dust: using near-IR camera arrays and subtracting these from optical CCD images. This method measures the dust extinction cross section and does not require the knowledge of dust temperature (see Block 1996; Block et al. 1994a,b, 1999). Otherwise, a detailed radiative transfer treatment of the interaction of the dust with starlight (e.g. Popescu et al. 2000, Tuffs et al. 2004) together with a physical interstellar dust model (e.g. Li & Draine 2001b,2002c) is required.

6. Can Dust Get Down to 2.7 K and Appear in Absorption against the CMB?

Ultrasmall grains spend most of their time at their vibrational ground state during the interval of two photon absorption events (§3 and Fig. 2; Draine & Li 2001). In the 1996 South African *"Cold Dust"* Symposium, it was heatedly argued that these grains could obtain a vibrational temperature less than the 2.7 K

temperature of the CMB so that they could be detected in absorption against the CMB (Duley & Poole 1998). However, based on detailed modeling of the excitation and de-excitation of these grains, we found that even though these grains do have a large population in the vibrational ground state, nevertheless the vibrational levels are sufficiently excited that the grains would appear in emission against the CMB with brightness temperature $\lesssim 9\,\mathrm{K}$ (see Draine & Li 2004b for details).

Acknowledgments I thank G.J. Bendo, D.L. Block, F. Boulanger, B.T. Draine, R.C. Kennicutt, J.I. Lunine, D. Pfenniger, J.L. Puget, M.W. Regan, and C. Yuan for helpful discussions. I am grateful to D.L. Block and the organizing committee for inviting me to this stimulating symposium. I also thank my advisors B.T. Draine and the late J.M. Greenberg for guiding me to this fascinating field – cosmic dust.

Notes

1. Struve & Elvey (1938) appear to be first to show that the interstellar gas is mostly hydrogen.

2. Let interstellar grains be approximated by a single size of a (spherical radius) with a column density of $N_{\rm d}$. The gas-to-dust mass ratio is

$$\frac{m_{\rm gas}}{m_{\rm dust}} \approx \frac{\left(\mu_{\rm H} + [{\rm He/H}]_{\rm ISM}\ \mu_{\rm He}\right)\ N_{\rm H}}{(4/3)\,\pi a^3 \rho_{\rm d} N_{\rm d}} \approx \frac{1.4 \mu_{\rm H}\, N_{\rm H}}{(4/3)\,\pi a^3 \rho_{\rm d} N_{\rm d}} \tag{2}$$

where $\mu_{\rm H}$ and $\mu_{\rm He}$ are respectively the atomic weight of H and He; $[{\rm He/H}]_{\rm ISM}$ is the interstellar He abundance (relative to H), which is taken to be that of the solar value, ~ 0.1; $\rho_{\rm d}$ is the mass density of interstellar dust. The hydrogen (of all forms)-to-dust column density $N_{\rm H}/N_{\rm d}$ can be derived from

$$\frac{N_{\rm H}}{E(B-V)} = \frac{N_{\rm H}}{A_V/R_V} = \frac{R_V\, N_{\rm H}}{1.086\,\pi a^2 Q_{\rm ext}(V)\, N_{\rm d}} \tag{3}$$

where R_V is the total-to-selective extinction ratio, $Q_{\rm ext}(V)$ is the dust extinction efficiency at V-band ($\lambda = 5500$ A). Therefore, the gas-to-dust ratio can be readily estimated from

$$\frac{m_{\rm gas}}{m_{\rm dust}} \approx 1.14\,\mu_{\rm H}\,\frac{Q_{\rm ext}(V)}{a\rho_{\rm d}}\,\frac{1}{R_V}\,\frac{N_{\rm H}}{E(B-V)} \approx 212\,\left(\frac{Q_{\rm ext}[V]}{1.5}\right)\left(\frac{0.1\,\mu{\rm m}}{a}\right)\left(\frac{2.5\,{\rm g\,cm^{-3}}}{\rho_{\rm d}}\right)\ . \tag{4}$$

If we take canonical numbers of $R_V \approx 3.1$, $Q_{\rm ext}(V) \approx 1.5$, $a = 0.1\,\mu$m, $\rho_{\rm d} \approx 2.5\,{\rm g\,cm^{-3}}$, $m_{\rm gas}/m_{\rm dust}$ would be around 210.

3. In our Milky Way Galaxy, interstellar matter (gas and dust; $7 \pm 3 \times 10^9 {\rm M}_\odot$), contributes roughly $\sim 20\%$ of the total stellar mass ($4 \pm 2 \times 10^{10} {\rm M}_\odot$). Therefore, the mass fraction of interstellar dust is just $\sim 0.1\%$ in our Galaxy ($\sim 1 \pm 0.2 \times 10^{11} {\rm M}_\odot$ within 10 kpc, Kennicutt 2001)!

4. In this method, the wavelength dependence of interstellar extinction is obtained by comparing the spectra of two stars of the same spectral type, one of which is reddened and the other unreddened.

5. Falco et al. (1999) found $R_V \approx 1.5$ for an elliptical lensing galaxy at $z_l \approx 0.96$, and $R_V \approx 7.2$ for a spiral lensing galaxy at $z_l \approx 0.68$. Wang et al. (2004) found the extinction curves for two intervening quasar absorption systems at $z \approx 1.5$ to have $R_V \approx 0.7, 1.9$.

6. For example, there is at least one line of sight (Sk 143=AvZ 456) with an extinction curve with a strong 2175A hump detected (Lequeux et al. 1982; Prevot et al. 1984; Bouchet et al. 1985; Thompson et al. 1988; Gordon & Clayton 1998). This sightline passes through the SMC wing, a region with much weaker star formation (Gordon & Clayton 1998). The sight lines which show no 2175A hump all pass through the SMC Bar regions of active star formation (Prevot et al. 1984; Gordon & Clayton 1998).

7. Strong regional variations in extinction properties have also been found in the LMC (Clayton & Martin 1985; Fitzpatrick 1985,1986; Misselt, Clayton, & Gordon 1999): the sightlines toward the stars inside or near the supergiant shell, LMC 2, which lies on the southeast side of the 30 Dor star-forming region, have very weak 2175 A hump (Misselt et al. 1999).

8. Kemper, Vriend & Tielens (2004) found that crystalline fraction of the interstellar silicates along the sightline towards the Galactic Center is $\sim 0.2\%$.

9. The amount of Si (relative to H) required to deplete in dust to account for the observed $9.7\,\mu$m feature strength is

$$\left[\frac{\rm Si}{\rm H}\right] = \frac{\Delta\tau_{9.7\,\mu{\rm m}}}{N_{\rm H}}\frac{1}{\kappa_{\rm sil}^{\rm abs}(9.7\,\mu{\rm m})\,\mu_{\rm sil}} = \frac{\Delta\tau_{9.7\,\mu{\rm m}}}{A_V}\frac{A_V}{N_{\rm H}}\frac{1}{\kappa_{\rm sil}^{\rm abs}(9.7\,\mu{\rm m})\,\mu_{\rm sil}} \tag{5}$$

where $\kappa_{\rm sil}^{\rm abs}(9.7\,\mu{\rm m})$ is the silicate mass absorption coefficient at λ=9.7 μm; $\mu_{\rm sil}$ is the silicate molecular weight. With $\kappa_{\rm sil}^{\rm abs}(9.7\,\mu{\rm m})\approx 2850\,{\rm cm^2\,g^{-1}}$ and $\mu_{\rm sil}\approx 172\mu_{\rm H}$ for amorphous olivine $MgFeSiO_4$, the local diffuse ISM ($\Delta\tau_{9.7\,\mu{\rm m}}/A_V\approx 1/18.5$, $A_V/N_{\rm H}\approx 5.3\times10^{-22}\,{\rm mag\,cm^2}$) requires $\left[\frac{\rm Si}{\rm H}\right]\approx 35\,{\rm ppm}$.

10. Hough et al. (1996) reported the detection of a weak 3.47 μm polarization feature in the Becklin-Neugebauer object in the OMC-1 Orion dense molecular cloud, attributed to carbonaceous materials with diamond-like structure. See Li (2004a) and Jones & d'Hendecourt (2004) for a detailed discussion on interstellar diamond.

11. Other C–H out-of-plane bending modes at 11.9, 12.7 and 13.6 μm have also been detected. The wavelengths of the C–H out-of-plane bending modes depend on the number of neighboring H atoms: 11.3 μm for solo-CH (no adjacent H atom), 11.9 μm for duet-CH (2 adjacent H atoms), 12.7 μm for trio-CH (3 adjacent H atoms), and 13.6 μm for quartet-CH (4 adjacent H atoms).

12. Li & Draine (2002b) have modeled the excitation of PAH molecules in UV-poor regions. It was shown that the astronomical PAH model provides a satisfactory fit to the UIR spectrum of vdB 133, a reflection nebulae with the lowest ratio of UV to total radiation among reflection nebulae with detected UIR band emission (Uchida, Sellgren, & Werner 1998).

13. Let $[{\rm X/H}]_\odot$ be the interstellar abundance of X relative to H (we assume interstellar abundances to be those of the solar values: $[{\rm C/H}]_\odot\approx 391$ parts per million [ppm], $[{\rm O/H}]_\odot\approx 501$ ppm, $[{\rm Mg/H}]_\odot\approx 34.5$ ppm, $[{\rm Fe/H}]_\odot\approx 34.4$ ppm, and $[{\rm Si/H}]_\odot\approx 28.1$ ppm [Sofia 2004]); $[{\rm X/H}]_{\rm gas}$ be the amount of X in gas phase ($[{\rm C/H}]_{\rm gas}\approx 130$ ppm, $[{\rm O/H}]_{\rm gas}\approx 375$ ppm; Fe, Mg and Si are highly depleted in dust: $[{\rm Fe/H}]_{\rm gas}\approx 1$ ppm, $[{\rm Mg/H}]_{\rm gas}\approx 2$ ppm, and $[{\rm Si/H}]_{\rm gas}\approx 2$ ppm [Sofia 2004]); $[{\rm X/H}]_{\rm dust}$ be the amount of X contained in dust ($[{\rm C/H}]_{\rm dust}=[{\rm C/H}]_\odot - [{\rm C/H}]_{\rm gas}\approx 261$ ppm, $[{\rm O/H}]_{\rm dust}\approx 126$ ppm, $[{\rm Mg/H}]_{\rm dust}\approx 32.5$ ppm, $[{\rm Fe/H}]_{\rm dust}\approx 27.1$ ppm, $[{\rm Si/H}]_{\rm dust}\approx 32.4$ ppm). Assuming H/C=0.5 for interstellar carbon dust, the gas-to-dust mass ratio is

$$\frac{m_{\rm gas}}{m_{\rm dust}} \approx \frac{1.4\,\mu_{\rm H}}{\sum_{\rm X}[{\rm X/H}]_{\rm dust}\,\mu_{\rm X}} \approx 165\,. \tag{6}$$

where the summation is over Si, Mg, Fe, C, O and H, and $\mu_{\rm X}$ is the atomic weight of X in unit of $\mu_{\rm H}\approx 1.66\times10^{-24}$ g.

14. Assuming all Si, Mg, and Fe elements of solar abundances are condensed in silicate dust of a stoichiometric composition $MgFeSiO_4$ with a characteristic size $a\approx 0.1\,\mu$m, the contribution of the silicate dust to the optical extinction is

$$\begin{aligned}\left(\frac{A_V}{N_{\rm H}}\right)_{\rm sil} &\approx 1.086\,\pi a^2 Q_{\rm ext}(V) N_{\rm sil}/N_{\rm H}\\ &\approx \frac{1.086\,\pi a^2 Q_{\rm ext}(V)\left(\sum_{\rm X=Si,Mg,Fe}[{\rm X/H}]_\odot\,\mu_{\rm X} + 4\,[{\rm Si/H}]_\odot\,\mu_{\rm O}\right)\mu_{\rm H}}{(4/3)\,\pi a^3\rho_{\rm sil}}\\ &\approx 3.2\times10^{-22}\,{\rm mag\,cm^2}\,.\end{aligned} \tag{7}$$

where $N_{\rm sil}$ is the column density of silicate dust, $\rho_{\rm sil}\approx 3.5\,{\rm g\,cm^3}$ is the mass density of silicate material, and $Q_{\rm ext}(V)$ is the visual extinction efficiency of submicron-sized silicate dust which is taken to be $Q_{\rm ext}(V)\approx 1.5$.

15. The idea of transient heating of very small grains was first introduced by Greenberg (1968). This process was not observed until many years later when the detection of the near-IR emission of reflection nebulae (Sellgren, Werner, & Dinerstein 1983) and detection by IRAS of 12 and 25 μm Galactic emission (Boulanger & Perault 1988) were reported.

16. This is because for large grains individual photon absorption events occur relatively frequently and the grain energy content is large enough that the temperature increases induced by individual photon absorptions are relatively small.

17. Li & Draine (2002c) placed an upper limit of $\sim 0.4\%$ of the SMC C abundance on the amount of PAHs in the SMC Bar. But we note that the PAH emission features have been seen in SMC B1#1, a quiescent molecular cloud (Reach et al. 2000). For this region, Li & Draine (2002c) estimated that $\sim 3\%$ of the SMC C abundance to be incorporated into PAHs.

18. Siebenmorgen et al. (1999) argued that the dust embedded in UV-attenuated clouds within the optical disk of typical inactive spiral galaxies cannot become colder than ~ 6 K.

References

Adamson, A.J., Whittet, D.C.B., Chrysostomou, A., Hough, J.H., Aitken, D.K., Wright, G.S., & Roche, P.F. 1999, ApJ, 512, 224

Aitken, D.K., Roche, P.F., Smith, C.H., James, S.D., & Hough, J.H. 1988, MNRAS, 230, 629

Allamandola, L.J., & Hudgins, D.M. 2003, in Solid State Astrochemistry, ed. V. Pirronello, J. Krelowski, & G. Manico (Dordrecht: Kluwer), 251

Allamandola, L.J., Tielens, A.G.G.M., & Barker, J.R. 1985, ApJ, 290, L25

Allamandola, L.J., Hudgins, D.M., & Sandford, S.A. 1999, ApJ, 511, L115

Andersen, A.C., Sotelo, J.A., Niklasson, G.A., & Pustovit, V.N. 2004, see **WCD04**, 709

Anderson, C.M., et al. 1996, AJ, 112, 2726

Bakes, E.L.O., & Tielens, A.G.G.M. 1994, ApJ, 427, 822

Barnard, E.E. 1919, ApJ, 49, 1

Bendo, G.J., et al. 2003, AJ, 125, 2361

Block, D.L. 1996, see **BG96**, 1

Block, D.L., & Greenberg, J.M., ed., 1996, New Extragalactic Perspectives in the New South Africa (Dordrecht: Kluwer) (hereafter **BG96**)

Block, D.L., Puerari, I., Frogel, J.A., Eskridge, P.B., Stockton, A., & Fuchs, B. 1999, Ap&SS, 269, 5

Block, D.L., Bertin, G., Stockton, A., Grosbol, P., Moorwood, A.F.M., & Peletier, R.F. 1994a, A&A, 288, 365

Block, D.L., Witt, A.N., Grosbol, P., Stockton, A., & Moneti, A. 1994b, A&A, 288, 383

Bohlin, R.C., Savage, B.D., & Drake, J.F. 1978, ApJ, 224, 132

Boogert, A.C.A., & Ehrenfreund, P. 2004, see **WCD04**, 547

Bouchet, P., Lequeux, J., Maurice, E., Prevot, L., & Prevot-Burnichon, M. L. 1985, A&A, 149, 330

Boulanger, F., & Perault, M. 1988, ApJ, 330, 964

Boulanger, F., Bourdin, H., Bernard, J.P., & Lagache, G. 2002, in EAS Publ. Ser., Vol. 4, Infrared and Submillimeter Space Astronomy, ed. M. Giard, J.P. Bernard, A. Klotz, & I. Ristorcelli (Paris: EDP Sciences), 151

Bowey, J.E., & Adamson, A.J. 2002, MNRAS, 334, 94

Cardelli, J.A., Clayton, G.C., & Mathis, J.S. 1989, ApJ, 345, 245

Chiar, J.E., Pendleton, Y.J., Geballe, T.R., & Tielens, A.G.G.M. 1998, ApJ, 507, 281

Chiar, J.E., et al. 2000, ApJ, 537, 749

Chini, R., Krugel, E., Lemke, R., & Ward-Thompson, D. 1995, A&A, 295, 317

Chrysostomou, A., Hough, J.H., Whittet, D.C.B., Aitken, D.K., Roche, P. F., & Lazarian, A. 1996, ApJ, 465, L61

Clayton, G.C., & Martin, P.G. 1985, ApJ, 288, 558
Clayton, G.C., et al. 1992, ApJ, 385, L53
Cohen, R.D., Burbidge, E.M., Junkkarinen, V.T., Lyons, R.W., & Madejski, G. 1999, BAAS, 31, 942
Dale, D.A., Helou, G., Contursi, A., Silbermann, N.A., & Kolhatkar, S. 2001, ApJ, 549, 215
Devereux, N.A., & Young, J.S. 1990, ApJ, 359, 42
Disney, M. 1996, see **BG96**, 21
d'Hendecourt, L.B., Léger, A., Olofson, G., & Schmidt, W. 1986, A&A, 170, 91
Douglas, A.E., & Herzberg, G. 1941, ApJ, 94, 381
Draine, B.T. 1990, in ASP Conf. Ser. 12, The Evolution of the Interstellar Medium, ed. L. Blitz (San Francisco: ASP), 193
Draine, B.T. 1999, in Proc. of the EC-TMR Conf. on 3K Cosmology, ed. L. Maiani, F. Melchiorri, & N. Vittorio (Woodbury: AIP), 283
Draine, B.T. 2003a, ARA&A, 41, 241
Draine, B.T. 2003b, in The Cold Universe, Saas-Fee Advanced Course Vol. 32, ed. D. Pfenniger (Berlin: Springer-Verlag), 213
Draine, B.T. 2004, see **WCD04**, 691
Draine, B.T., & Lee, H.M. 1984, ApJ, 285, 89
Draine, B.T., & Lazarian, A. 1998a, ApJ, 494, L19
Draine, B.T., & Lazarian, A. 1998b, ApJ, 508, 157
Draine, B.T., & Li, A. 2001, ApJ, 551, 807
Draine, B.T., & Li, A. 2004a, in preparation
Draine, B.T., & Li, A. 2004b, in preparation
Draine, B.T., & Tan, J.C. 2003, ApJ, 594, 347
Duley, W.W., & Poole, G. 1998, ApJ, 504, L113
Dumke, M., Krause, M., & Wielebinski, R. 2004, A&A, 414, 475
Dwek, E., Zubko, V., Arendt, R.G., & Smith, R.K. 2004, see **WCD04**, 499
Falco, E.E., et al. 1999, ApJ, 523, 617
Fitzpatrick, E.L. 1985, ApJ, 299, 219
Fitzpatrick, E.L. 1986, AJ, 92, 1068
Frisch, P.C., et al. 1999, ApJ, 525, 492
Galliano, F., Madden, S.C., Jones, A.P., Wilson, C.D., Bernard, J.-P., Le Peintre, F. A&A, 407, 159
Gordon, K.D. 2004, see **WCD04**, 77
Gordon, K.D., & Clayton, G.C. 1998, ApJ, 500, 816
Gordon, K.D., Witt, A.N., & Friedmann, B.C. 1998, ApJ, 498, 522
Greenberg, J.M. 1968, in Stars and Stellar Systems, Vol. VII, ed. B.M. Middlehurst, & L.H. Aller, (Chicago: Univ. of Chicago Press), 221
Greenberg, J.M., Li, A., Mendoza-Gómez, C.X., Schutte, W.A., Gerakines, P.A., & de Groot, M. 1995, ApJ, 455, L177
Grün, E., Gustafson, B.A.S., Mann, I., et al. 1994, A&A, 286, 915
Hartmann, J. 1904, ApJ, 19, 268
Henning, Th., Jäger, C., & Mutschke, H. 2004, see **WCD04**, 603
Hough, J.H., Chrysostomou, A., Messinger, D.W., Whittet, D.C.B., Aitken, D.K., & Roche, P.F. 1996, ApJ, 461, 902
Joblin, C., Léger, A., & Martin, P. 1992, ApJ, 393, L79
Jones, A.P., & d'Hendecourt, L.B. 2004, see **WCD04**, 589
Kemper, F., Vriend, W.J., & Tielens, A.G.G.M. 2004, ApJ, 609, 826
Kennicutt, R.C. 2001, in Tetons 4: Galactic Structure, Stars and the Interstellar Medium, ed. C.E. Woodward, M.D. Bicay, & J.M. Shull (San Francisco: ASP), 2

Koornneef, J., & Code, A.D. 1981, ApJ, 247, 860
Krügel, E. 2003, The Physics of Interstellar Dust (Bristol: IoP)
Krügel, E., Siebenmorgen, R., Zota, V., & Chini, R. 1998, A&A, 331, L9
Landgraf, M., Baggaley, W.J., Grün, E., Krüger, H., & Linkert, G. 2000, J. Geophys. Res., 105, 10343
Larson, K.A., Whittet, D.C.B., & Hough, J.H. 1996, ApJ, 472, 755
Ledoux, G., et al. 1998, A&A, 333, L39
Léger, A., & Puget, J.L. 1984, A&A, 137, L5
Lehtinen, K., & Mattila, K. 1996, A&A, 309, 570
Lequeux, J., & Jourdain de Muizon, M. 1990, A&A, 240, L19
Lequeux, J., Maurice, E., Prévot-Burnichon, M.-L., Prévot, L., & Rocca-Volmerange, B. 1982, A&A, 113, L15
Li, A. 2003a, ApJ, 584, 593
Li, A. 2003b, ApJ, 599, L45
Li, A. 2004a, in ASP Conf. Ser. 309, Astrophysics of Dust, ed. A.N. Witt, G.C. Clayton, & B.T. Draine (San Francisco: ASP), 417
Li, A. 2004b, to be submitted to ApJ
Li, A., & Draine, B.T. 2001a, ApJ, 550, L213
Li, A., & Draine, B.T. 2001b, ApJ, 554, 778
Li, A., & Draine, B.T. 2002a, ApJ, 564, 803
Li, A., & Draine, B.T. 2002b, ApJ, 572, 232
Li, A., & Draine, B.T. 2002c, ApJ, 576, 762
Li, A., & Greenberg, J.M. 1997, A&A, 323, 566
Li, A., & Greenberg, J.M. 1998, A&A, 339, 591
Li, A., & Greenberg, J.M. 2002, ApJ, 577, 789
Li, A., & Greenberg, J.M. 2003, in Solid State Astrochemistry, ed. V. Pirronello, J. Krelowski, & G. Manicò (Dordrecht: Kluwer), 37
Malhotra, S. 1997, ApJ, 488, L01
Martin, P.G., & Whittet, D.C.B. 1990, ApJ, 357, 113
Martin, P.G., Clayton, G.C., & Wolff, M.J. 1999, ApJ, 510, 905
Martin, P.G., et al. 1992, ApJ, 392, 691
Mathis, J.S. 1996, ApJ, 472, 643
Mathis, J.S., Mezger, P.G., & Panagia, N. 1983, A&A, 128, 212
Mathis, J.S., Rumpl, W., & Nordsieck, K.H. 1977, ApJ, 217, 425
Mattila, K., et al. 1996, A&A, 315, L353
McKellar, A. 1940, PASP, 52, 187
Mennella, V., Brucato, J.R., Colangeli, L., & Palumbo, P. 1999, ApJ, 524, L71
Mennella, V., et al. 2001, A&A, 367, 355
Misselt, K.A., Clayton, G.C., & Gordon, K.D. 1998, ApJ, 515, 128
Motta, V., et al. 2002, ApJ, 574, 719
Muñoz Caro, G.M., Ruiterkam, R., Schutte, W.A., Greenberg, J.M., & Mennella, V. 2001, A&A, 367, 347
Nandy, K., Morgan, D.H., Willis, A.J., Wilson, R., & Gondhalekar, P. M. 1981, MNRAS, 196, 955
Onaka, T., et al. 1996, PASJ, 48, L59
Pendleton, Y.J. 2004, see **WCD04**, 573
Pendleton, Y.J., & Allamandola, L.J. 2002, ApJS, 138, 75
Pendleton, Y.J., Tielens, A.G.G.M., & Werner, M.W. 1990, ApJ, 349, 107
Pendleton, Y.J., Sandford, S.A., Allamandola, L.J., Tielens, A.G.G.M., & Sellgren, K. 1994, ApJ, 437, 683

Popescu, C.C., Misiriotis, A., Kylafis, N.D., Tuffs, R.J., Fischera, J. 2000, A&A, 362, 138
Popescu, C.C., Tuffs, R.J., Völk, H.J., Pierini, D., & Madore, B.F. 2002, ApJ, 567, 221
Prévot, M.L., Lequeux, J., Prevot, L., Maurice, E., & Rocca-Volmerange, B. 1984, A&A, 132, 389
Purcell, E.M. 1969, ApJ, 158, 433
Reach, W.T., Boulanger, F., Contursi, A., & Lequeux, J. 2000, A&A, 361, 895
Reach, W.T., et al. 1995, ApJ, 451, 188
Regan, M.W., et al. 2004, ApJS, 154, 204
Schnaiter, M., Henning, Th., & Mutschke, H. 1999, ApJ, 519, 687
Schutte, W.A., et al. 1998, A&A, 337, 261
Sellgren, K., Rouan, D., & Léger, A. 1988, A&A, 196, 252
Sellgren, K., Werner, M.W., & Dinerstein, H.L. 1983, ApJ, 271, L13
Siebenmorgen, R., Krügel, E., & Chini, R. 1999, A&A, 351, 495
Smith, J.D., et al. 2004, ApJS, 154, 199
Smith, T.L., & Witt, A.N. 2002, ApJ, 565, 304
Snow, T.P., & Witt, A.N. 1996, ApJ, 468, L65
Sofia, U.J. 2004, see **WCD04**, 393
Stecher, T.P. 1965, ApJ, 142, 1683
Struve, O. 1929, MNRAS, 89, 567
Struve, O., & Elver, C.T. 1938, ApJ, 88, 364
Swings, P., & Rosenfeld, L. 1937, ApJ, 86, 483
Tanaka, M., et al. 1996, PASJ, 48, L53
Thompson, G.I., Nandy, K., Morgan, D.H., & Houziaux, L. 1988, MNRAS, 230, 429
Toft, S., Hjorth, J., & Burud, I. 2000, A&A, 357, 115
Trumpler, R.J. 1930, PASP, 42, 214
Tuffs, R.J., Popescu, C.C., Völk, H.J., Kylafis, N.D., & Dopita, M.A. 2004, A&A, 419, 821
Uchida, K.I., Sellgren, K., & Werner, M.W. 1998, ApJ, 493, L109
Wang, J., Hall, P.B., Ge, J., Li, A., & Schneider, D.P. 2004, ApJ, 609, 589
Weingartner, J.C., & Draine, B.T. 2001a, ApJ, 548, 296
Weingartner, J.C., & Draine, B.T. 2001b, ApJS, 134, 263
Whittet, D.C.B. 2003, Dust in the Galactic Environment (2nd ed; Bristol: IoP)
Witt, A.N., & Vijh, U.P. 2004, see **WCD04**, 115
Witt, A.N., Bohlin, R.C., & Stecher, T.P. 1986, ApJ, 305, L23
Witt, A.N., Clayton, G.C., & Draine, B.T., ed., 2004, ASP Conf. Ser. 309, Astrophysics of Dust (San Francisco: ASP) (hereafter **WCD04**)
Witt, A.N., Gordon, K.D., & Furton, D.G. 1998, ApJ, 501, L111
Witt, A.N., Smith, R.K., & Dwek, E. 2001, ApJ, 550, L201
Witt, A.N., Lindell, R.S., Block, D.L., & Evans, R. 1994, ApJ, 427, 227
Wolff, M.J., Clayton, G.C., Kim, S.H., Martin, P.G., & Anderson, C.M. 1997, ApJ, 478, 395
Zubko, V.G., Dwek, E., & Arendt, R.G. 2004, ApJS, 152, 211